JOINT INSTITUTE
FOR NUCLEAR RESEARCH

Analysis and Interactive Visualization of Neutrino Event Topologies Registered in the OPERA Experiment

Author: Khalid Hassouna

Ph.D. student, University of Hawaii at Manoa
Hawaii, USA

Supervisor: Dr. Sergey Dmitrievsky

Researcher,Joint Institute for Nuclear Research
Dubna, Russia

July, 2022

Contents

Abstract

The longstanding solar neutrino problem, as well as atmospheric neutrino anomaly, led to the discovery of neutrino oscillations. OPERA experiment aimed to establish neutrino oscillations in direct appearance mode in the $\nu_\mu \rightarrow \nu_\tau$ channel, through the detection of the short-lived tau lepton. A search procedure is developed to search for the tau particle by studying the decay topology and comparing it with the Monte-Carlo simulated data. Finally, the candidate events are visualized by tracing the track lines and the detector hits in 2-dimensional and 3-dimensional web applications.

Part I

Theory

Chapter 1

Introduction to Neutrinos

1.1 Neutrinos in the standard model

The standard model, being the most successful theoretical framework for elementary particles, classified the elementary particles according to their roles in the interaction of three of the four fundamental forces (Gravity is the only fundamental force that is not yet integrated into the model on the experimental level. Thus, it doesn't impact the classification imposed by the standard model on the particles). The model has two main classes: bosons and fermions. The former includes the forces' carriers while the latter encompasses the elementary particles that compose normal matter.

The main distinction between fermions and bosons is their statistical behavior. Bosons are particles that have integer spin while fermions have half-odd-integer spin. Following this spin difference, fermions abide by the Pauli-exclusion principle and on the contrary, bosons can violate it. This principle and the corresponding statistics based on it are taken as an empirical result in the classical theory of quantum mechanics; nevertheless, it can be proven from fundamental principles in the modern approach of quantum field theory.

The fermionic matter is then sub-classified into quarks and leptons. Among some differences that differentiate between quarks and leptons, the most significant one is that the latter is subject to interaction under the strong force; however, the latter is neutral regarding it.

Neutrinos belong to the lepton family. The family is divided into 3 generations and consists of a total of 6 particles. The generations differ

from each other in the flavor quantum number and the mass [1]. The first generation includes the electron (e) and the electron neutrino (ν_e). The second generation contains the muon particle (μ) and the muon neutrino (ν_μ). Finally, the third generation consists of the tau particle (τ) and the tau neutrino (ν_τ). Figure (1.1) summarizes the structure of the standard model.
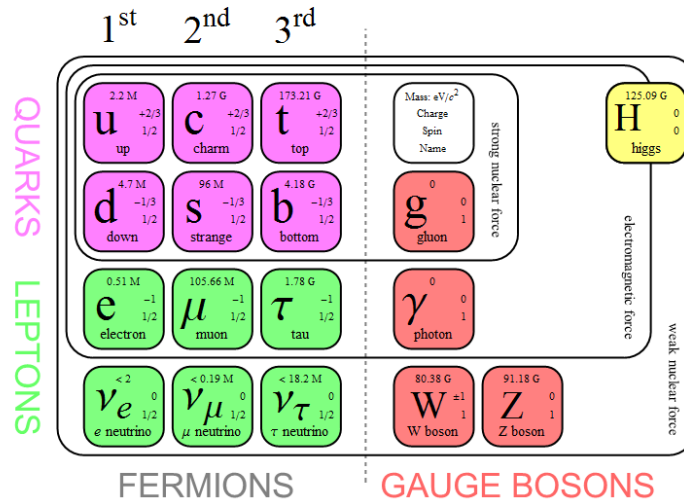

Figure 1.1: The standard model

1.2   Neutrinos history

The story began in 1911 when Lise Meitner and Otto Hahn performed an experiment that resulted in an apparent contradiction to the conservation law of energy. Hahn and Meitner studied the energy spectrum of the electrons emitted by beta decay that turned out to be continuous rather than discrete [1]. Electrons are distributed in discrete orbits around the nucleus which give them a discrete energy spectrum. This discreteness must continue when the electrons are emitted by the beta decay; however, the results of Hahn and Meitner showed that the spectrum is continuous in a direct contradiction to the theoretical expectation based on the conservation of energy. Moreover, the spin of the Nitrogen-14 atom was discovered experimentally to be 1 violating Rutherford's expectation that it is $\frac{1}{2}$ [2]. At this time, it was clear that either, there is a fundamental problem with the conservation laws we have at hand like the conservation of energy or there is some missing

---

[1]neutrinos are excepted from the mass criterion because the mass of neutrinos is not yet fully understood. More about this in the next sections

explanation. The first possibility is not on the scope of the viable options for first, the conservation of energy is a fundamental law tested millions of times with modern science based on it, and secondly, for the way the law is formulated. Conservation of energy arises as a result of the continuous symmetry of time by Noether's theorem. Violating this rule suggests that space-time is not homogeneous which would cause more complications.

The solution came from Wolfgang Pauli when he, in 1930, in a letter sent to the radioactive community that was gathered for a conference in Tubingen city in Germany, suggested that atoms, in addition to protons and electrons, also contain another guest particle that he initially called "the neutron" [2]. This ghost particle was later named "neutrino" by Fermi in 1933 and it was assumed to carry energy and momentum to explain the missing energy in the beta decay. It was also aspired to have spin $\frac{1}{2}$ to explain the spin 1 of Nitrogen-14 [2]. In the letter written by Pauli, he suggested that neutrinos, as later named by Fermi, are different from the light quanta by having a mass on the order of the electron mass. Thus, they can't travel at the speed of light. However, this assumption of neutrinos being massive needed many decades to witness light. It emerged as a solution to the solar problem to be discussed in the next section. The first experimental proof of the existence of neutrinos came in 1956 by Reines and Cowan [4]. This was followed by the second family of neutrinos and the third one in 1962 and 1975 respectively. [2].

Three flavors of neutrinos are enough to be accommodated in consistence with the standard model. This is because neutrinos are attached to flavors from the other 3 leptons and they carry their names. This happens because whenever neutrinos interact, their partner particles show up. Neutrinos' weak interactions are classified into 2 categories: charged-current (CC) interactions and neutral-current interactions (NC). The classification depends on the boson involved in the interaction. If the boson is the charged $W^{\pm}$, the interaction is CC. On the other hand, if the boson is the neutral Z boson, the interaction is NC. An illustrative diagram is shown in figure (1.3). The important feature to derive from the figure is that Whenever the neutrino ν_i interacts, the lepton partner l_i appears where i $\in$ {e, μ, τ}.

Figure 1.2: Wolfgang Pauli

---

[2]It might sound confusing that Pauli chose a name that is associated with another particle, but the point is that James Chadwick made his discovery of the currently named neutrons in 1932, 2 years after Pauli's letter and was awarded Nobel prize for this discovery in 1935 [3].
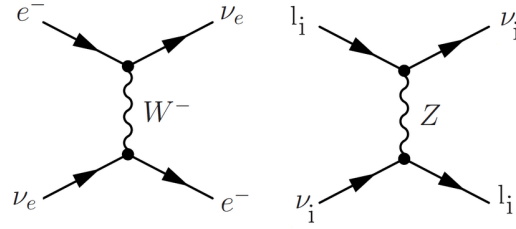
Figure 1.3: Feynman diagrams of CC and NC interactions of neutrinos [5, p.26]

1.3   The solar neutrino problem and neutrinos oscillation

The sun is the nearest star to the earth and hence it is the most intense source of stellar neutrinos. Neutrinos of different energies are produced in fusion reactions that take place in the sun. Neutrinos are produced in several chain reactions. The main ones are summarized as follows [6], **Proton-Proton-chain (PP-chain):**

$$p + p \rightarrow d + e^+ + \nu_e \tag{1.1}$$

$$^8B \rightarrow {}^8Be^* + e^+ + \nu_e \tag{1.2}$$

$$e^- + {}^7Be \rightarrow {}^7Li + \nu_e \tag{1.3}$$

pep-process & **hep-process:** The contribution from this chain to energy production is in order of KeV's. Thus, the energy contribution is very low; however, it contributes on a non-negligible order to neutrinos production.

$$p + p + e^- \rightarrow d + \nu_e \tag{1.4}$$

$$p + {}^3\text{He} \rightarrow {}^4\text{He} + e^+ + \nu_e \tag{1.5}$$

CNO cycle (Carbon-Nitrogen-Oxygen Cycle): This cycle produces less than 9% of the sun's energy [7].

$$^{13}N \rightarrow {}^{13}C + \beta^+ + \nu_e \tag{1.6}$$

$$^{15}O \rightarrow {}^{15}C + \beta^+ + \nu_e \tag{1.7}$$

$$^{17}F \rightarrow {}^{17}C + \beta^+ + \nu_e \tag{1.8}$$

If equation (1.1) is multiplied by 2, it becomes,

$$4p \rightarrow 2d + 2e^+ + 2\nu_e$$

The 2 deuterons fuse together to give 4-Helium and excess energy and the equation becomes,

$$4p \rightarrow 4\text{He} + 2\text{e}^+ + 2\nu_e \tag{1.9}$$

The left-hand side of equation (1.9) is heavier than the right-hand side and hence there is a lot of energy released in this reaction for which this equation was regarded as the biggest source of the energy emitted from the sun to earth that eventually reaches the earth in the form of sunlight. Additionally, equation (1.9) and the other chains and processes emitting neutrinos show that the only neutrinos emitted from the are electron neutrinos. The other two flavors can be produced in accelerators or in other exploding stars where the heavier particles, muon, and tau, are produced. In the reactions discussed above, only the electron showed up among the other leptons and hence the only emitted neutrino was the electron neutrino.

In 1964, John Bashall and Raymond Davis Jr. constructed an experiment to test if really, equation (1.9) is the main source of sunlight. The experiment has a tank, the size of about a swimming pool, filled with chlorine-based cleaning fluid (C_2Cl_4). As the sun emits electron neutrinos; when these neutrinos interact with $^{3}7Cl$, they would turn them into radioactive argon atoms $^{3}7Ar$. The problem is that neutrinos interact very weakly and hence they had to wait for several months to get a few atoms of Argon. The result was that the observed Argon atoms are about one-third of the expected amount [7, 8]. This is known as the solar neutrino problem.

The solution came as a violation of the old formulation of the electroweak theory in the standard model given by Glashow, Weinberg, and Salam which suggested that the flavor is conserved. The detection process in Davis and Bashall's experiment was devoted to electron neutrino only; nevertheless, as neutrinos travel over a distance, they oscillate changing their flavor. Therefore, the electron starting as an electron neutrino might later change to muon neutrino or tau neutrino. This happens because neutrinos are created in flavor eigenstates, but they travel in mass eigenstates. The two eigenbases are different from each other, so the best to do is to write the flavor eigenstate as a linear combination of the mass eigenstates.The flavor eigenstates are written as ν_α where $\alpha \in \{e, \mu, \tau\}$ and the mass eigenstates are written as ν_i where $i \in \{1, 2, 3\}$ with mass m_i [9].

$$\nu_\alpha = \sum_i U_{\alpha i} \nu_i$$

where U is a 3×3 unitary matrix known as the PMNS matrix named after Pontecorvo, Maki, Nakagawa, and Sakata. It can be decomposed as,

$$U \equiv \begin{pmatrix} 1 & 0 & 0 \\ 0 & \cos\theta_{23} & \sin\theta_{23} \\ 0 & -\sin\theta_{23} & \cos\theta_{23} \end{pmatrix} \begin{pmatrix} \cos\theta_{13} & 0 & \sin\theta_{13}e^{-i\delta} \\ 0 & 1 & 0 \\ -\sin\theta_{13}e^{i\delta} & 0 & \cos\theta_{13} \end{pmatrix}$$

$$\begin{pmatrix} \cos\theta_{12} & \sin\theta_{12} & 0 \\ -\sin\theta_{12} & \cos\theta_{12} & 0 \\ 0 & 0 & 1 \end{pmatrix},$$

As neutrinos travel, the mass eigenstates pick different phases, and hence their linear combination changes and they no longer represent the initial flavor eigenstate. This is known as neutrino oscillation. This solution was also proof that neutrinos are not massless as it was long thought.

Chapter 2

OPERA experiment

2.1 Introduction

The OPERA experiment was designed to find an experimental proof for $\nu_\mu \to \nu_\tau$ oscillation in the appearance mode. The detection relied on the unique signature of ν_τ CC interaction with the final state of τ-particle. The tau particle is a short-lived particle and its decay is categorized into four main decay channels (muon, electron, or hadron) or 3 prongs. Prongs have an electric charge of ± 1 and the tau particle has a charge of negative one. Thus, it can decay only to an odd number of prongs. The main ones are 1 and 3; nevertheless, it can still decay to 5 or 7....etc. prongs, but these are neglected as they contribute with a very low branching fraction to the decay.

2.2 Experiment details

A pure muon neutrino beam was directed from the source located at CERN to the detector located at the underground Gran Sasso Laboratory (LNGS). The beam was called CNGS (CERN neutrinos to Gran Sasso, CNGS). The average neutrino energy was 17 GeV, and the traveled distance between the source and the detector was 730 Km. The contamination was in the form of 2.1% of $\bar{\nu}_\mu$, 1% of $\bar{\nu}_e$ and ν_e, and a negligible $O(10^{-7})$ contamination from ν_τ [10].

2.3 The detector

The detector was made of nuclear emulsions interleaved with lead plates as a target of a total mass of about 1.25 kt equipped with electronic detectors.

The general structure had 2 identical super modules (SM) each of which was composed of 31 target walls and a muon spectrometer. Each target wall had target units loaded on horizontal trays. The target units are known as bricks. Each brick had 57 nuclear emulsion films with 56 lead plates with a thickness of $300\mu m$ for the former and $1\mu m$ for the latter. There were 2 orthogonal planes of scintillator strips that functioned as target tracker detectors to record the position and energy deposition of charged particles. The last component was the spectrometer used to identify muons and measure their momentum [10]. A Full description of the detector instrumentation is given in [11]. The decay search procedure is well-explained in [12, p.3-6].
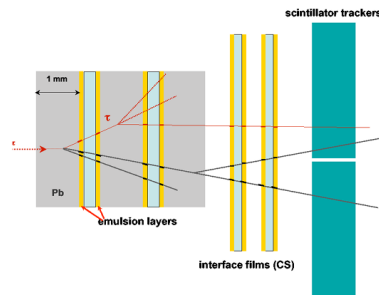

Figure 2.1: illustrative schematic diagram of ν_τ CC interaction and the decay of the tau particle as a final-state particle as it would appear in OPERA brick [11, p. 4]
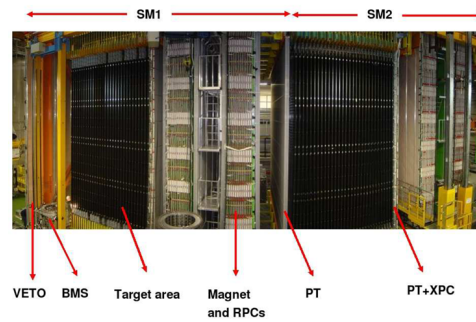

Figure 2.2: side view of OPERA detector [11, p. 5]

Part II

Data analysis

Chapter 3

Neutrino-induced charmed hadron production analysis

3.1 Introduction

The OPERA experiment developed a systematic analysis procedure to detect short-lived particles. This analysis procedure aimed to detect oscillated ν_τ CC interactions through the direct detection of the decay of the tau particle. The final state tau particle decaying into several decaying channels such as decaying to a muon, electron, hadron, or an odd number of prongs, especially 3 is a distinctive print of the ν_τ CC interactions which in return reveals $\nu_\mu \rightarrow \nu_\tau$ oscillation.

The analysis procedure can also be applied to the detection of ν_μ CC interaction with charmed hadrons as final state particles. In this chapter, instead of applying the analysis procedure to the detection of the tau particle, it is applied to detect charmed hadrons in a data sample of located ν_μ CC events.

The charmed particles represent a very powerful tool for cross-check the efficiency of detecting the tau particle because both of them show very similar decay topologies for having close masses and lifetimes.

In the light of this, the goal of this chapter is to analyze the decay topology, in the form of the decay length and the impact parameter, of a sample of charmed hadrons as final-state particles in real data of ν_μ CC interactions. Then, this real data is compared with Mote-Carlo simulated data to show the efficiency of reconstructing the ν_μ CC interaction. The details of the Monte Carlo simulation are discussed in [12].

3.2 Data sample

All the predicted CC events are analyzed from the data samples collected in 2008 and 2009 runs. For the data collected in the 2010 run, only the NC and CC events with the following conditions were considered:

- The events are reconstructed with a negative muon.

- A selection cut of maximum momentum 15 GeV/C is applied.

In total, the data sample included 2925 ν_μ CC events out of which 50 decay candidate events of charmed hadrons as final-state particles are observed.

3.3 Decay length

The decay length is the length of the distance traveled by the charmed hadron before decay. The charmed hadron is created at the primary vertex of ν_μ CC interaction and the decay takes place at the secondary vertex according to the set-up convention. The positions of the primary and the secondary vertices

	Standard	Standard	Standard	Standard	Standard	Standard	Standard
1	vertType	posX	posY	posZ	globPosX	globPosY	globPosZ
2	1	16412.8	60392.9	41863.8	182.09	-122.85	220.87
3	2	16453.7	60437.1	42414.9	182.09	-122.85	220.92

Figure 3.1: Example of the retrieved data in CSV file of vertices positions

are given in CSV files in the form `id_Vertices.csv` where the part `"id"` takes a number specific to each vertex of the 50 observed events in the emulsion data for neutrino-induced charmed hadron production studies [13] as in figure (3.1).

The aim is to develop a Python code to compute the distance between 2 points (the primary and secondary vertices) in 3 dimensions from the 50 CSV files (the number of decay candidate events of charmed hadrons as final-state particles) and then store this data in a histogram using ROOT [1]. The flight length is computed by the simple equation,

$$d = \sqrt{(x_1 - x_2)^2 + (y_1 - y_2)^2 + (z_1 - z_2)^2} \qquad (3.1)$$

An illustrative diagram of the decay is shown in figure (3.2). The result of the analysis is given in figure (3.3) (length is given in μm). Figure (3.8) shows the results concluded in [12] after an analysis run on real data along with a comparison with the Monte-Carlo simulated data. All the histograms, either run on real data or Monte-Carlo simulation, show similar behavior which indicates a high performance of the detector and the analysis procedure to detect short-lived particles. The histogram of this project has a little

---

[1] https://github.com/Khalid570/Charmed-hadrons-topology

deviation from the histogram shown in [12] and the reason is that the data used in this project is uploaded on CERN open data in 2020 while [12] was published in 2014. Thus, this time difference causes the laboratories around the world working on the OPERA experiment to update their data with improvements and hence change the data and the results a little bit; however, both histograms show similar behavior and are in good agreement with the Monte-Carlo simulated data.
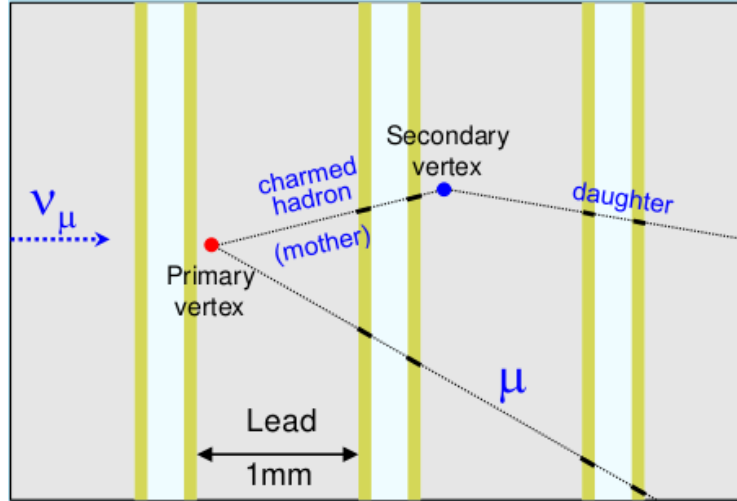

Figure 3.2: Charmed hadron decay in ν_μ CC interaction
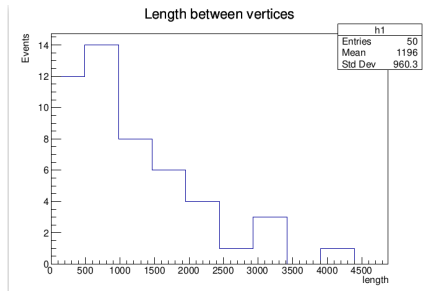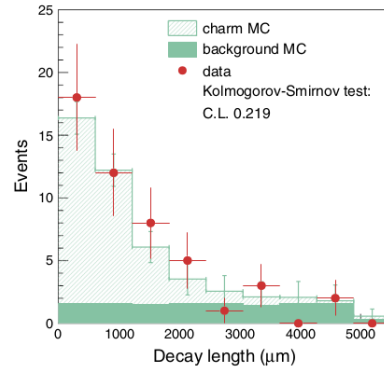

Figure 3.3: decay length histogram

Figure 3.4: [12, p.8]

3.4 Impact parameter

The other topological feature that is of interest for the decay of charmed hadrons is the impact parameter. The impact parameter is the perpendicular distance between the daughter particle track and the primary vertex of ν_μ CC interaction.

As the charmed hadron decays, it emits daughter particles that take specific tracks. Each track represents a straight line in 3 dimensions. To specify a straight line in 3-d, it is required to have 2 points to be able to draw a vector from one point to the other.Two points along each track line associated with a secondary vertex are given in a CSV file in the form `id_Vertices.csv`

	Standard	Standard	Standard	Standard	Standard	Standard	Standard
1	trType	posX1	posY1	posZ1	posX2	posY2	posZ2
2	9	109886.1	43564.0	15169.4	109843.9	43598.1	15688.5
3	1	109886.1	43564.0	15169.4	110238.4	44102.8	21669.4
4	10	109843.9	43598.1	15688.5	109717.9	43777.9	19588.5
5	10	109843.9	43598.1	15688.5	109684.0	43760.3	19588.5
6	2	109886.1	43564.0	15169.4	109903.7	43500.8	19069.4

Figure 3.5: Example of the retrieved data in CSV file of track line positions

where the part `"id"` takes a number specific to each vertex of the 50 observed events in the emulsion data for neutrino-induced charmed hadron production studies [13] as in figure (3.5). The track type of daughter particles has the number "10" and it is possible to have more than one daughter particle for one charmed hadron as in figure (3.5). Each CSV file of the track lines has its corresponding CSV file of vertices. The goal is to calculate the impact parameter for each track line of a daughter particle with respect to the primary vertex.
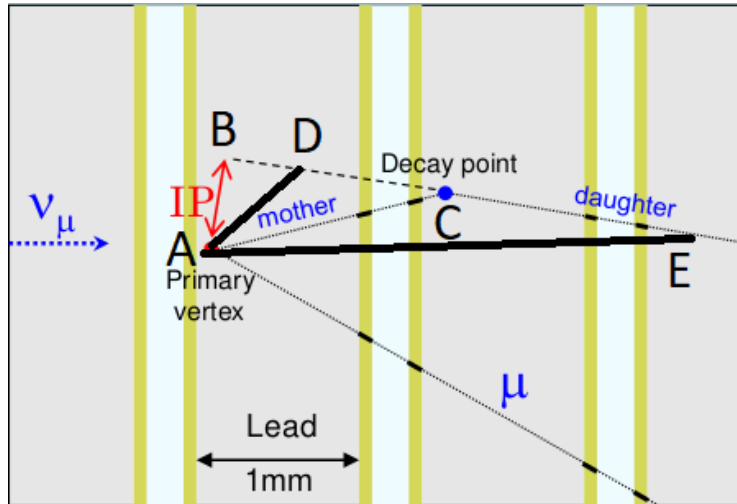

Figure 3.6: Impact parameter of a daughter particle in a charmed-hadron decay resulting from ν_μ CC interaction.

Refer to figure (3.7). The location of point B is not known, but it is possible to know the direction of the vector $\vec{BC}$ by subtracting the two points given in the CSV file along the track line of the daughter particle; they are the points D and E in the figure. These two points in the CSV file are not necessarily the points B and C as in figure (3.7) [2], but they lie on the same track line and hence their subtraction gives the same vector direction (not magnitude) as the one given by subtracting D and E. $\hat{BC} = \hat{DE}$

To recap, the location of point B is not given. On the other hand, the locations of the points D and E are known; they are the points along the track lines of the daughter particles as given in the CSV files. Additionally, location of point A is known because this is the primary vertex given in the CSV files of the vertices discussed in the previous section.

$$|\vec{AB}| = |\vec{AE}|sin(\angle AEB)$$
$$sin(\angle AEB) = \frac{\vec{AE} \times \vec{DE}}{|\vec{AE}||\vec{DE}|}$$

$$|\vec{AB}| = \frac{\vec{AE} \times \vec{DE}}{|\vec{DE}|} \tag{3.2}$$

A Python code is developed to calculate the vectors $\vec{AE}$ and $\vec{DE}$ for each primary vertex. Then, equation 3.2 is applied to calculate the impact parameter for every daughter particle. A total of 91 daughter particles is observed and so, 91 impact parameters are calculated. The data is then saved into a histogram using ROOT (Refer to the same GitHub repository as the one for decay length.). The histogram is shown in figure (3.7).

As in the previous section, the data in [12] is compared with the Monte-Carlo simulation showing a high level of agreement indicating a high level of success of the analysis procedure searching for short-lived particles as final state particles and especially, the charmed hadrons which exhibit similar decaying topology to the one shown by the tau particle. Once, again, there is a slight difference between the histogram built in this project and the one used in [12] for the time difference and the slight difference in the used data, but the general trend is still the same.

---

[2]In our specific case the points C and D are identical, but, in principle, they could be different.
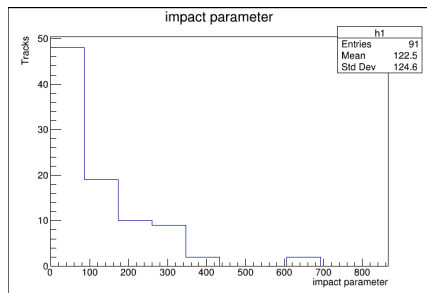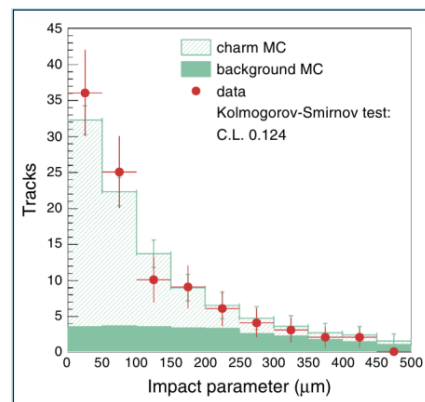
Figure 3.7: impact parameter histogram

Figure 3.8: [12, p.8]

Chapter 4

Analysis of the track lines

4.1 Introduction

The study of the topological characteristics of the track lines of hadronic final states continues. In this chapter, two more topological features are analyzed:

- The multiplicity distribution of charged hadrons in hard scattering processes.

- Angles of the muon tracks emerging from the primary vertices of ν_μ CC interactions.

The study of the multiplicity distribution is of high significance in the hard scattering process, so it was highly analyzed in several collision experiments [14, 15, 16].

4.2 Data sample

Between 2008 and 2012, OPERA collected data on an order of 1.8×10^{20}. From these data, 19505 neutrino interaction events were recorded by the electronic detectors. The search for the primary vertex put a selection cut that reduced the number of events to 5603. 4406 out of the 5603 located events had an identified muon. The analysis is run on a chosen unbiased sub-sample of 817 events occurring in the lead with a negatively charged muon spotted by the muon spectrometer [17]. The details of the selection cuts can be found in [18].

4.3 Multiplicity distribution of charged hadrons

Track multiplicity is defined to be the number of track lines (different charged particles, like muons, electrons, or hadrons) emerging from a given vertex (In our case, it is the primary vertex of the ν_μ CC interaction). The emulsion data for track multiplicity is

	Standard	Standard	Standard	Standard	Standard	Standard	Standard	Standard	Standard
1	evID	timestamp	posX	posY	posZ	globPosX	globPosY	globPosZ	mult
2	10150031630	1275190030000	32299.1	86168.6	56342	-87.0345	227.185	-510.858	2

Figure 4.1: Example of the retrieved data in CSV file of vertices multiplicities and positions

given in CSV files in the form `id_Vertex.csv` where the part `"id"` takes a number specific to each vertex of the 817 observed events [19]. A Python code is developed to read the multiplicity from every CSV file and store the data in a histogram using ROOT [1]. The result is shown in figure (4.2).A similar analysis was carried out in [17] with a slight deviation in the used data. As in the previous chapter, the two histograms show a high level of agreement with each other and also with the Monte-Carlo simulated data indicating a high-level performance from the detectors.
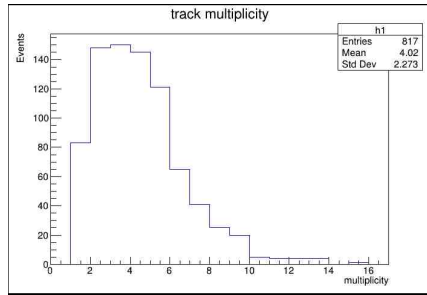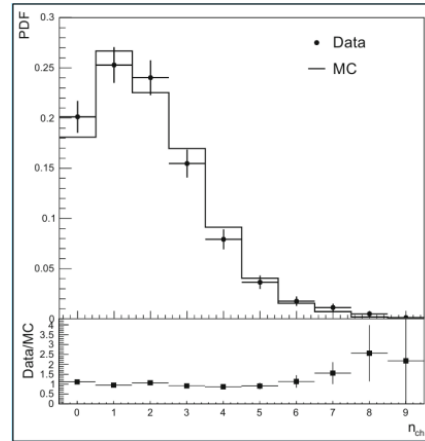

Figure 4.2: multiplicity histogram

Figure 4.3: [17, p.5]

4.4 Angles of muon track lines

To identify a track line in 3 dimensions, it is sufficient to locate a point that is taken to be the primary vertex or a point near to it for experimental uncertainty and 2 angles that are taken to be the angles made in XZ and YZ planes. The emulsion data for the slopes and the

	Standard	Standard	Standard	Standard	Standard	Standard
1	trType	posX	posY	posZ	slopeXZ	slopeYZ
2	2	54013.8	41362.6	25878	-0.0591	-0.0154
3	2	54028.2	41394.9	25878	-0.026	0.0314
4	2	54046.8	42019.7	27168	0.0038	0.337
5	1	53928.8	41356.3	25878	-0.1869	-0.036

Figure 4.4: Example of the retrieved data in CSV file of the slopes made by the track lines

---

[1] https://github.com/Khalid570/multiplicities-angles-distribution.git

primary vertex or the point near to it are given in CSV files in the form
`id_Tracks.csv` where the part `"id"` takes a number specific to each vertex of
the 817 observed events [19]. The interest in this analysis section is confined
to the muon track lines that have `trType` $= 1$. The angles made with the
X-axis and Y-axis are calculated using the fact that slopeXZ/YZ $=$ tan(angle
made with the X/Y-axis).

$$\phi(\text{angle made with the X/Y-axis}) = tan^{-1}(slopeXZ/YZ) \qquad (4.1)$$

A Python code is developed to read the slopes from the CSV files, calculate
the angles made with the X and Y axes using equation (4.1) and draw a
2-dimensional histogram of the distribution of the angles using matplotlib
module [2]. The result is shown in figure (4.5). The same distribution is shown
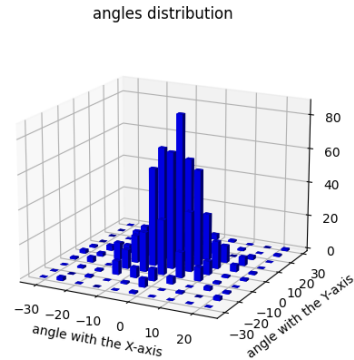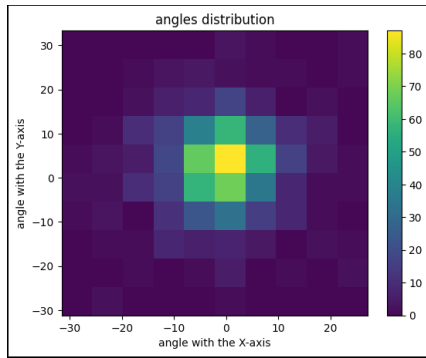in figure (4.6) with a 3-dimensional projection.

Figure 4.5: 2-dimensional histogram of the angles distribution of the muon track lines emerging from ν_μ CC interaction

Figure 4.6: 3-dimensional projection of a 2-dimensional histogram of the angles distribution of the muon track lines emerging from ν_μ CC interaction

---

[2] https://github.com/Khalid570/multiplicities-angles-distribution.git

Part III

Visualization

Chapter 5

Visulaization of the tau neutrino candidates

5.1   Introduction

Using the data discussed in section (4.2), an analysis was run to detect the tau-lepton particle through the identification of its decay topology. Kinematical selection cuts were applied to reduce the background decays that exhibit similar topological features as the one exhibited by the tau lepton. The background noise comes from three main sources[10]:

   I. Charmed hadrons decay emerging from ν_μ CC interactions..

  II. Re-interaction of hadrons in ν_μ CC interactions.

 III. Large-angle scattering of muons.

(I) was discussed in section (3.1) as a useful and powerful tool to cross-check the efficiency of the detectors to detect the tau lepton because they exhibit a similar decay topology; however, this comes with the drawback that it also causes a background noise when detecting the tau lepton. The selection cuts are determined based on the decay channel. The tau lepton has 4 main decay channels ($\tau \to e$, $\tau \to \mu$, $\tau \to 1h$, $\tau \to 3h$) where h is a charged hadron. A full discussion of the background reduction and the selection cuts is given in [10].

Following a series of kinematical cuts on the topological characteristics and parameters, in 2015, 5 ν_τ candidates were observed. This came up with the experimental detection of $\nu_\mu \to \nu_\tau$ oscillation with a significance of 5.1σ [20]. In 2018, this result was updated to 10 ν_τ candidates with a significance of 6.1σ using looser selection criteria [21].

5.2 Tracks and vertices reconstructed in nuclear emulsions

The emulsion data for tau neutrino appearance studies [22] gives CSV files in the forms `id_Vertices.csv` and `id_Lines.csv` where the part `"id"` takes a number specific to each event. The former specifies the position of the vertices and the latter specific two points along the track lines to be able to recover the whole track. The strategy is to extract and read off the data associated with the ν_τ candidates and save it to JavaScript structures. Then, with the help of the THREE.js graphics library, an Html file is written to build a simplified version of a browser-based 3D event display of the vertices and the track lines of the 10 tau neutrino candidate events [1]. The results are shown for 4 examples out of the 10 candidate events in figures (5.1, 5.2, 5.3, 5.5).
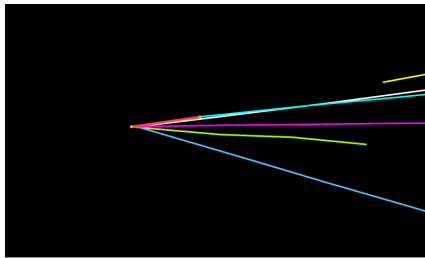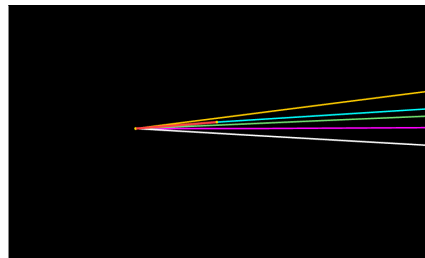

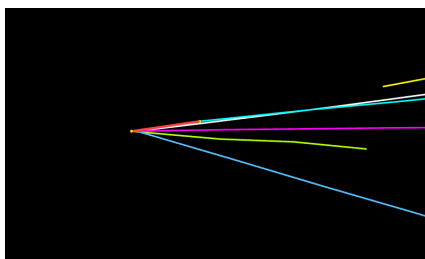Figure 5.1: Event 11143018505

Figure 5.2: Event 11172035775

Figure 5.3: Event 11213015702

Figure 5.4: Event 12123032048

---

[1]https://github.com/cernopendata/demobbed-viewer.git
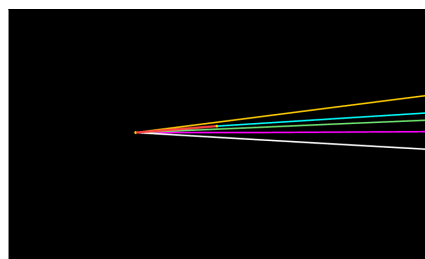
5.3   Electronic detector hits

The electronic detector data for tau neutrino appearance studies [23] is given in the form of CSV files that contain data about the positions of target tracker (TT) hits, RPC, and drift tubes (DT) hits in XZ and YZ projections for the ten tau neutrino candidate events. The strategy is to extract and read off the data associated with the ν_τ candidates and save it to JavaScript structures. Then, with the help of the D3.js graphics library, an Html file is written to build a simplified version of a browser-based 2D event display of the electronic detector hits [2]. The results are shown for 4 examples out of the 10 candidate events in figures (5.5, 5.6, 5.7, 5.8).
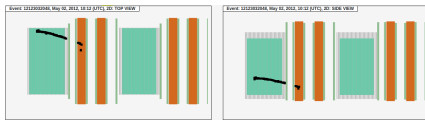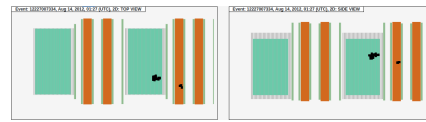

Figure 5.5: Event 12123032048

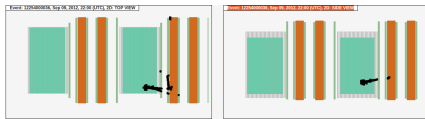
Figure 5.6: Event 12227007334

Figure 5.7: Event 12254000036

Figure 5.8: Event 11113019758

---

[2]https://github.com/cernopendata/demobbed-viewer.git
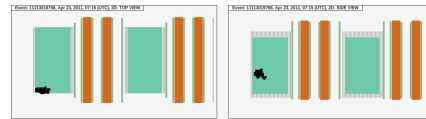
Conclusion

The report was divided into 3 parts. In part 1, a theoretical basis was built up for how neutrinos were integrated into the standard model and their historical background. Then, the solar neutrino problem was described which, among others, led to the discovery of the neutrino oscillation phenomenon.

This phenomenon is the core of the OPERA experiment which detected the oscillation of muon neutrino into tau neutrino $\nu_\mu \to \nu_\tau$. The detection comes from the detection of the tau particle; however, this particle is short-lived and its detection comes from tracing its decay topology.

In part 2, the decay topology of charmed hadrons was studied. The charmed hadrons exhibit a similar decay topology to the one exhibited by the tau particle and hence they can serve as a cross-check test for the efficiency of the experiment. Furthermore, the multiplicity distribution of hadrons and the angles distribution of the muon tracks were analyzed for the ν_μ CC interaction. The study of the multiplicity distribution and the scattering angles distribution of the muons was very important in 2 points: first, it reveals much about the interaction dynamics which is very important in reconstructing the candidate events and secondly, the large scattering angles might be a source of background noise when reconstructing the tau neutrino candidate events and hence it helps in setting the kinematical selection cuts. All the analysis run on the real data was compared with Monte-Carlo simulated data which showed good agreement indicating a high performance of the detectors.

Part 3 was about visualizing the track lines and the vertices of the tau neutrino candidate events and the electronic detector hits.

Bibliography

[1] O. V. Bayer, O. Hahn, and L. Meitner, *Phys. Zeitschr.*, vol. 273, 1911.

[2] "1931 – Pauli presents hypothetical "neutron" particle." [Online]. Available: https://icecube.wisc.edu/neutrino-history/1931/01/1931-pauli-presents-hypothetical-neutron-particle/

[3] "James Chadwick Biographical." [Online]. Available: https://www.nobelprize.org/prizes/physics/1935/chadwick/biographical/

[4] F. Reines and Clyde L.Cowan, "The Neutrino," *nature*, vol. 178, pp. 446–449, 1956. [Online]. Available: https://doi.org/10.1038/178446a0

[5] D. Lietti and M. Prest, "The Electron Muon Ranger for the MICE Experiment," 08 2022.

[6] N. Hawkins, "The Solar Neutrino Problem," 04 2017.

[7] R. Davis, D. S. Harmer, and K. C. Hoffman, "Search for neutrinos from the sun," *Phys. Rev. Lett.*, vol. 20, pp. 1205–1209, May 1968. [Online]. Available: https://link.aps.org/doi/10.1103/PhysRevLett.20.1205

[8] J. N. Bahcall, "Solving the mystery of the missing neutrinos," 04 2004. [Online]. Available: https://www.nobelprize.org/prizes/themes/solving-the-mystery-of-the-missing-neutrinos/

[9] Y. Farzan and M. Tórtola, "Neutrino oscillations and non-standard interactions," *Front. Phys.*, Feb 2018. [Online]. Available: https://www.frontiersin.org/articles/10.3389/fphy.2018.00010/full#B1

[10] N.Agafonova *et al.*, "Final results of the opera experiment on ν_τ appearance in the cngs neutrino beam," *Phys. Rev. Lett.*, vol. 120, p. 211801, 2018. [Online]. Available: https://link.aps.org/doi/10.1103/PhysRevLett.120.211801

[11] R. Acquafredda *et al.*, "The OPERA experiment in the CERN to gran sasso neutrino beam," *Journal of Instrumentation*, vol. 4, no. 04, pp. P04 018–P04 018, apr 2009. [Online]. Available: https://doi.org/10.1088/1748-0221/4/04/p04018

[12] N.Agafonova *et al.*, "Procedure for short-lived particle detection in the OPERA experiment and its application to charm decays," *The European Physical Journal C*, vol. 74, 2014. [Online]. Available: https://link.springer.com/article/10.1140/epjc/s10052-014-2986-0

[13] "Emulsion data for neutrino-induced charmed hadron production studies," 2019. [Online]. Available: https://opendata.cern.ch/record/13101

[14] R.E.Ansorge *et al.*, "Charged particle multiplicity distributions at 200 and 900 Gev c.m. energy," *Z. Phys. C - Particles and Fields*, vol. 43, pp. 357–374, 1989. [Online]. Available: https://link.springer.com/article/10.1007/BF01506531

[15] G.J.Alner *et al.*, "UA5: A general study of proton-antiproton physics at $\sqrt{s}$=546 GeV," *Physics Reports*, vol. 154, no. 5, pp. 247–383, 1987. [Online]. Available: https://www.sciencedirect.com/science/article/pii/037015738790130X

[16] P.Allen *et al.*, "Multiplicity distributions in neutrino-hydrogen interactions," *Nuclear Physics B*, vol. 181, no. 5, pp. 385–402, 1981. [Online]. Available: https://doi.org/10.1016/0550-3213(81)90532-0

[17] N.Agafonova *et al.*, "Study of charged hadron multiplicities in charged-current neutrino–lead interactions in the OPERA detector," *The European Physical Journal C*, vol. 78, 2018. [Online]. Available: https://link.springer.com/article/10.1140/epjc/s10052-017-5509-y

[18] N.Agafonova *et al.*, "Study of charged hadron multiplicities in charged-current neutrino-lead interactions in the OPERA detector," *Journal of High Energy Physics*, vol. 11, 2013. [Online]. Available: https://www.researchgate.net/publication/317932031_Study_of_charged_hadron_multiplicities_in_charged-current_neutrino-lead_interactions_in_the_OPERA_detector

[19] "Emulsion data for track multiplicity," 2018. [Online]. Available: https://opendata.cern.ch/record/3901

[20] N. Agafonova *et al.*, "Discovery of τ neutrino appearance in the cngs neutrino beam with the opera experiment," *Phys. Rev. Lett.*, vol. 115, p. 121802, Sep 2015. [Online]. Available: https://link.aps.org/doi/10.1103/PhysRevLett.115.121802

[21] N. Agafonova *et al.*, "Opera tau neutrino charged current interactions," *Sci Data*, vol. 8, 2021. [Online]. Available: https://doi.org/10.1038/s41597-021-00991-y

[22] "Emulsion data for tau neutrino appearance studies," 2018. [Online]. Available: https://opendata.cern.ch/record/10001

[23] "Electronic detector data for tau neutrino appearance studies," 2018. [Online]. Available: https://opendata.cern.ch/record/10000